Available online at www.sciencedirect.com
SCIENCE DIRECT®
Biochimica et Biophysica Acta 1617 (2003) 96–108
BIOCHIMICA ET BIOPHYSICA ACTA
BBA
www.bba-direct.com

The F–G loop region of cytochrome P450scc (CYP11A1) interacts with the phospholipid membrane

Madeleine J. Headlam[a,1], Matthew C.J. Wilce[b], Robert C. Tuckey[a,*]

[a] *Department of Biochemistry and Molecular Biology, School of Biomedical and Chemical Sciences, University of Western Australia, 35 Stirling Highway, Crawley, WA 6009, Australia*
[b] *Department of Crystallography, School of Biomedical and Chemical Sciences, University of Western Australia, Crawley, WA 6009, Australia*

Received 1 July 2003; received in revised form 16 September 2003; accepted 23 September 2003

Abstract

Cytochrome P450scc (CYP11A1) is a protein attached to the inner surface of the inner mitochondrial membrane that uses cholesterol from the membrane phase as its substrate for the first step in steroid hormone synthesis. We investigated the mechanism by which CYP11A1 interacts with the membrane. Hydrophobicity profiles of CYP11A1 and two other mitochondrial cytochromes P450, plus a model structure of CYP11A1 using CYP2C5 as template, suggest that CYP11A1 has a monotopic association with the membrane which may involve the A′ helix and the F–G loop. Deletion of the A′ helix reduced the proportion of expressed CYP11A1 associated with the bacterial membrane fraction, indicating a role for the A′helix in membrane binding. However, introduction of a cysteine residue in this helix at position 24 (L24C) and subsequent labelling with the fluorescent probe *N*′-(7-nitrobenz-2-oxal,3-diazol-4-yl)ethylenediamine (NBD) failed to show a membrane localisation. Cysteine mutagenesis and fluorescent labelling of other residues appearing on the distal surface of the CYP11A1 model revealed that V212C and L219C have enhanced fluorescence and a blue shift following association of the mutant CYP11A1 with phospholipid vesicles. This indicates that these residues, which are located in the F–G loop, become localised to a more hydrophobic environment following membrane binding. Analysis of the quenching of tryptophan residues in CYP11A1 by acrylamide indicates that at least one and probably two tryptophans are involved in membrane binding. We conclude that CYP11A1 has a monotopic association with the membrane that is mediated, at least in part, by the F–G loop region.

Keywords: Cytochrome P450scc; CYP11A1; Membrane; Fluorescence; Pregnenolone; Phospholipid vesicle

1. Introduction

Cytochrome P450 side chain cleavage (CYP11A1) catalyses the initial and rate-limiting step of steroid hormone synthesis, the conversion of cholesterol to pregnenolone. Cholesterol has extremely low solubility in water and appears to be transferred to the active site of CYP11A1 from the inner mitochondrial membrane to which the CYP11A1 is bound [1]. Determining the nature of the interaction of CYP11A1 with the membrane is therefore necessary to understand the catalytic mechanism and could provide information for subsequent modification of the membrane domain to facilitate protein crystallisation and structure determination. CYP11A1 is the best characterised of the mitochondrial P450 enzymes with a large number of published observations on the physical and catalytic properties of the enzyme. It therefore provides an excellent model for structure–function studies of mitochondrial type cytochromes P450.

Electron spin resonance studies have provided evidence that the heme group of CYP11A1 is roughly parallel to the plane of the membrane and is not embedded within the hydrophobic membrane environment [2,3]. Hydrophobicity profiles indicate that CYP11A1 lacks an N-terminal transmembrane anchor, a structural feature both predicted and identified for microsomal P450s [4,5]. It has been suggested that CYP11A1 is a transmembrane protein based on experiments using antibodies to probe membrane topology in mitochondria and using a transmembrane prediction algorithm [6,7]. This is in contrast to results from trypsinolysis experiments [8] as well as rotational diffusion and freeze-

* Corresponding author. Tel.: +61-8-9380-3040; fax: +61-8-9380-1148.
E-mail address: rtuckey@cyllene.uwa.edu.au (R.C. Tuckey).
[1] Current address: Research School of Chemistry, Australian National University, Canberra 0200, ACT, Australia.

0005-2736/$ - see front matter © 2003 Elsevier B.V. All rights reserved.
doi:10.1016/j.bbamem.2003.09.007

fracture analysis of liposomal CYP11A1, which indicate that CYP11A1 is tightly integrated but not transmembrane [9,10]. The N-terminal half of CYP11A1 remains associated with the mitochondrial membrane following partial tryptic digestion and sodium carbonate extraction while the C-terminal peptide is solubilised [11]. Removal of the N-terminal membrane-binding domain of an engineered microsomal CYP2C5 has resulted in the crystallisation and subsequent structure determination of the soluble domain of an eukaryotic P450 [12]. In addition to the hydrophobic N-terminal, there are likely to be other regions of membrane interaction for microsomal P450s [12–14]. The crystal structure of truncated CYP2C5 has surface residues mainly from the N-terminal that include the F–G loop, residues before the A helix and β strands 1–1 and 2–2 that may be part of a secondary membrane-binding site.

The reconstitution of CYP11A1 into artificial phospholipid vesicles provides a defined system for studying CYP11A1 membrane interactions and has been used in the present study. CYP11A1 incorporates into preformed vesicles spontaneously [15,16] and all of the reconstituted CYP11A1 molecules have an external adrenodoxin binding site [1] and a heme orientation that is similar to CYP11A1 in the mitochondrial membrane [2,3,17]. The reconstituted CYP11A1 can bind and metabolise cholesterol from within the vesicle bilayer [15,17,18]. In the present study we have investigated the membrane topology of CYP11A1 using methods of hydrophobicity profiling, secondary and tertiary structure prediction, site-directed cysteine mutagenesis and fluorescence spectroscopy. Our data reveal that residues within the F–G loop of CYP11A1 are embedded in the phospholipid membrane.

2. Materials and methods

2.1. Materials

Tris-(2-carboxyethyl)phosphine hydrochloride and *N*,*N*′-dimethyl-*N*-(iodoacetyl)-*N*′-(7-nitrobenz-2-oxa-1,3-diazol-4-yl)ethylenediamine (IANBD) were from Molecular Probes (Eugene, OR). The sources of other chemicals have been described [19].

2.2. Hydrophobicity profiles

A multiple sequence alignment was generated for bovine CYP11A1, human CYP11B1 and human CYP27A1 using the T-Coffee alignment method which is particularly suited to sequences of low identity [20]. The hydrophobicity profile for each of the above sequences was determined using the water to bilayer interfacial partitioning scale of Wimley and White [21]. The hydrophobicity profile and predicted membrane interfacial partitioning domains were generated with the program MPEx (http://blanco.biomol.uci.edu/mpex/index.html). The multiple alignment was then employed to generate a spreadsheet of the multiply aligned hydrophobicity profile for the cytochrome P450 enzymes.

2.3. Modelling of CYP11A1

To aid with model selection and sequence alignment, the secondary structure of CYP11A1 was predicted with ProteinPredict. Of the known P450 structures, CYP2C5 [12] has the highest sequence similarity to CYP11A1 with 21% identity and was used as the template for the CYP11A1 model. The major advantage of using this microsomal P450 structure is the fact that it is the only membrane-bound P450 with known soluble domain structure. The disadvantage is the lower resolution compared to the next most likely homologues of CYP108 and CYP102. The N-terminal hydrophobic anchor of CYP2C5 was deleted to aid crystallisation, but the protein was still associated with the membrane [22]. Poor homology exists between the N-terminal of CYP2C5 and CYP11A1 whereas CYP108 has similar secondary structure and length to that predicted for CYP11A1. We therefore used CYP108 (1CPT.pdb) as a structural template for the A′ and A helices. Usanov et al. [23] also used the N-terminal of CYP108 for their model of CYP11A1 which used CYP102 as the general template structure. Our model was generated using the Swiss Model automated server and the heme group was modelled into the heme-binding site by hand.

2.4. Mutagenesis and expression of bovine CYP11A1

Plasmid comprising the expression vector (pTrc99A) and cDNA encoding bovine CYP11A1 was constructed to contain coding sequence in a manner similar to that described by Wada and Waterman [24]. Mutagenesis was performed using the Quikchange™ site-directed mutagenesis kit (Stratagene) with mutagenesis primers shown in Table 1. The mutations were confirmed using automated Big-Dye Terminator DNA sequencing (Applied Biosystems).

The wild-type plasmid described above was modified by site-directed mutagenesis to substitute the one free cysteine residue (C264) to serine. Serine is found in this position for 40% of known mitochondrial P450 enzymes. This C264S mutant was then used as the template for subsequent site-directed cysteine mutagenesis. The primers for the C264S and subsequent cysteine mutants are listed in Table 1. Due to the large number of residues of the CYP11A1 model that are located on the distal side of the molecule, it was unfeasible to modify all residues for analysis of membrane interaction. We therefore made and analysed a number of selected cysteine mutants with the aim of spanning regions that might be associated with the membrane.

E. coli JM109 competent cells that had been prepared using the $RbCl_2$ method were transformed with the plasmid encoding wild-type or mutant CYP11A1 [25]. A freshly transformed isolate was prepared for expression culture as

Table 1
Oligonucleotides used to generate deletion and cysteine mutants of CYP11A1

Template	Mutation	Oligonucleotide
Wild type	A′ delete	5′-CTCCCCTGGTGACAATGGCGGCTCACAGAGAATCCACTTTCGCC-3′
		5′-GGCGAAAGTGGATTCTCTGTGAGCCGCCATTGTCACCAGGGGAG-3′
Wild type	C-terminal delete	5′-CGCCGGACAAGCCCTGATTCCTTGTCTTCCGCC-3′
		5′-GGCGGAAGACAAGGAATCAGGGCTTGTCCGGCG-3′
Wild type	C264S	5′-GGCATCCTCTACTCCCTCCTGAAAAGTGAG-3′
		5′-CTCACTTTTCAGGAGGGAGTAGAGGATGCC-3′
C264S	N23C	5′-CAATGGCTGGCTTTGCCTCTACCATTTCTGGAGG-3′
		5′-CCAGAAATGGTAGAGGCAAAGCCAGCCATTGTC-3′
C264S	L24C	5′-GGTGACAATGGCTGGCTTAACTGCTACCATTTCTGGAGG-3′
		5′-CTCCCTCCAGAAATGGTAGCAGTTAAGCCAGCCATTGTC-3′
C264S	H26C	5′-GGCTTAACCTCTACTGTTTCTGGAGGGAGAAGGG-3′
		5′-CTCCCTCCAGAAACACAGTAGAGGTTAAGCCAG-3′
C264S	N57C	5′-GAGAAGCTTGGCTGTTTGGAGTCAGTTTATATCATTCACC-3′
		5′-GATATAAACTGACTCCAAACACAGCCAAGCTTCTCCCTG-3′
C264S	L58C	5′-CAGGGAGAAGCTTGGCAATTGTGAGTCAGTTTATATCATTCAC-3′
		5′-CAGGGTGAATGATATAAACTGACTCACAATTGCCAAGCTTCTC-3′
C264S	S60C	5′-CTTGGCAATTTGGAGTGTGTTTATATCATTCACCCTGAAG-3′
		5′-GGTGAATGATATAAACACACTCCAAATTGCCAAGCTTC-3′
C264S	Y94C	5′-GGCTGGCCTATCACCGATGTTATCAGAAACCCATTGG-3′
		5′-GGACTCCAATGGGTTTCTGATAACATCGGTGATAGGCC-3′
C264S	Y200C	5′-CCAGAAGTTCATTGATGCCGTCTGCAAGATGTTCCACAC-3′
		5′-CACTGGTGTGGAACATCTTGCAGACGGCATCAATGAAC-3′
C264S	V212C	5′-GTGTCCCTCTGCTCAACTGCCCTCCTGAACTGTAC-3′
		5′-CGGTACAGTTCAGGAGGGCAGTTGAGCAGAGGGAC-3′
C264S	L219C	5′-CCTCCTGAACTGTACCGTTGTTTCAGAACCAAGACTTGGAG-3′
		5′-CCTCCAAGTCTTGGTTCTGAAACACGGTACAGTTCAGGAG-3′
C264S	V229C	5′-CCAAGACTTGGAGGGACCATTGTGCCGCATGGGACAC-3′
		5′-GTGTCCCATGCGGCACAATGGTCCCTCCAAGTCTTGG-3′
C264S	D233C	5′-CCATGTAGCCGCATGGTGCACAATTTTCAATAAAGCTG-3′
		5′-CAGCTTTATTGAAAATTGTGCACCATGCGGCTACATGG-3′
C264S	T234C	5′-GCATGGGACTGTATTTTCAATAAAGCTGAAAAATACACTGAGATC-3′
		5′-CTTTATTGAAAATACACGTCCCATGCGGCTACATGG-3′
C264S	N237C	5′-CACAATTTTCTGTAAAGCTGAAAAATACACTGAGATCTTCTACCAGG-3′
		5′-GTGTATTTTTCAGCTTTACAGAAAATTGTGTCCCATGCGGC-3′
C264S	T243C	5′-CAATAAAGCTGAAAAATACTGTGAGATCTTCTACCAGG-3′
		5′-GGTAGAAGATCTCACAGTATTTTTCAGCTTTATTGAAAATTGTG-3′
C264S	L460C	5′-GACGTGGACACCATATTCAACTGCATCCTGACGCCGG-3′
		5′-GCTTGTCCGGCGTCAGGATGCAGTTGAATATGGTGTCC-3′
C264S	L470C	5′-GGACAAGCCCATCTTCTGTGTCTTCCGCCCCTTC-3′
		5′-GAAGGGGCGGAAGACACAGAAGATGGGCTTGTC-3′

described [26]. Terrific broth was inoculated (1:50) with the Luria Bertani culture and grown as previously described except the expression time was shortened to 48 h for the deletion mutants [27].

2.5. Purification of CYP11A1 from bovine adrenals and E. coli

Native CYP11A1 was purified from bovine adrenals as described previously [28]. The expressed wild-type enzyme and the mutants were extracted from *E. coli* with 1% Emulgen 913 and the insoluble debris was separated [29]. The detergent was then adsorbed to Amberlite XAD-2 (1.5 × 25 cm at flow 1 ml/min for 100-ml extract) equilibrated with 20 mM potassium phosphate (pH 7.4), 20 mM sodium chloride, 20% glycerol (Buffer A), containing 1 mM DTT, 0.1 mM EDTA and CYP11A1 was collected in the flow through. The enzyme solution was concentrated using an Amicon concentrator with YM10 membrane and purified by adrenodoxin Sepharose affinity chromatography [29]. Eluted enzyme was dialysed at 4 °C against 50 mM potassium phosphate (pH 7.4), 50 mM sodium chloride, 20% glycerol, 0.03% cholate and 0.1 mM tris-(2-carboxyethyl)phosphine hydrochloride, concentrated and stored substrate free at − 80 °C. Cytochrome P450 concentrations were determined from carbon monoxide reduced minus reduced absorption spectra [30].

2.6. Cholesterol side chain cleavage assay

The activity of the CYP11A1 cysteine mutants incorporated into small unilamellar vesicles was determined at 37 °C using 0.03 μM CYP11A1, 10 μM adrenodoxin and 0.3 μM adrenodoxin reductase as described previously [19]. Vesicles were prepared from dioleoyl phosphatidylcholine, cholesterol and cardiolipin in a molar ratio of 1:0.4:0.15.

The amount of pregnenolone produced was measured by radioimmunoassay [31].

2.7. Distribution of CYP11A1 mutants between soluble and membrane fractions

For analysis of the localisation of deletion mutants, the *E. coli* cells were harvested, lysed and separated into a soluble fraction, a membrane fraction and inclusion bodies [32]. Protein content for the soluble and membrane fractions and inclusion bodies were determined using a Lowry assay [33]. Two modifications were made to maintain solubility and to miniaturise the assay to volumes suitable for microtitre plate wells. The assay was scaled to 250-μl final volume and 1% SDS was included. The introduction of SDS did not alter the sensitivity of the assay with bovine serum albumin used as standard. The wild-type and mutant protein fractions were separated by SDS-polyacrylamide gel electrophoresis (SDS-PAGE) on a 7.5% gel, then transferred to a nitrocellulose membrane for Western blot analysis [34] using antiserum raised against bovine CYP11A1 [35]. Each fraction was analysed by densitometry to determine the relative amounts of immuno-reactive CYP11A1 using NIH Image 1.62. One set of triplicate samples within the linear range of the Western blot was used for the densitometric analysis for each experiment.

2.8. Quenching of tryptophan fluorescence

To investigate whether any of the tryptophan residues found in native CYP11A1 were associated with the membrane, we tested the ability of acrylamide to quench the fluorescence before and after CYP11A1 insertion into vesicle membranes. Vesicles were prepared from egg phosphatidylcholine, cholesterol and cardiolipin in a molar ratio of 1:0.2:0.15, by bath sonication as described previously [19]. Vesicle-associated CYP11A1 was prepared in buffer (pH 7.4) comprising 50 mM potassium phosphate, 130 mM sodium chloride and 75 μM phospholipid. Aqueous or vesicle-associated CYP11A1 (0.5 mM) was excited at 295 nm and fluorescence was measured for the emission wavelengths of 310 to 400 nm using a scan speed of 120 nm/min with a Cary Eclipse fluorescence spectrophotometer (Varian). Excitation and emission bandwidths were set to 5 nm and temperature was maintained at 20 °C in a stirred quartz cuvette with path length of 5 mm. Emission scans were corrected for scatter by subtraction of buffer or vesicles as appropriate. Acrylamide titrations were performed with fixed excitation of 295 nm and an emission wavelength of 335 nm, with 5-nm bandwidths. Tryptophan fluorescence of CYP11A1 was measured in the absence (F_0) and then in the presence (F) of increasing concentrations of acrylamide. Fluorescence intensity was corrected for absorbance by acrylamide as described previously [36] and for dilution due to added quencher. The absorbance at 295 nm did not exceed 0.07 during the titration. The quench constant (K_q) was determined using the Stern–Volmer plot from the following equation:

$$F_0/F = 1 + K_q[Q]$$

where F_0 is the initial fluorescence intensity and F is the intensity at each molar concentration of quencher [Q]. The fraction of accessible tryptophan residues was analysed using the Lehrer plot derived from a modified Stern–Volmer equation [37]:

$$F_0/\Delta F = 1/(fK_q[Q]) + 1/f$$

where ΔF is the change in fluorescence due to quenching and f is the fraction of initial fluorescence accessible to the quencher.

2.9. Fluorescent labelling of CYP11A1 mutants

Prior to fluorescent labelling, CYP11A1 mutants (40 nmol) were exchanged into buffer (pH 7.4) comprising 50 mM potassium phosphate and 100 mM sodium chloride, by gel filtration (G25 Sephadex, 0.75 × 20 cm). This removed the glycerol prior to reaction since it is known to alter the spin state and conformation of CYP11A1 and increase the melting temperature of proteins [19,38], which could inhibit labelling. All of the purified CYP11A1 mutants were stable for the duration of the experiments in the absence of glycerol. The CYP11A1 was then reacted with a 10-fold molar excess of IANBD at room temperature according to the manufacturer's instructions. The labelled CYP11A1 was purified by gel filtration using Buffer A containing 0.1% cholate and 1 mM EDTA, and loaded onto an adrenodoxin Sepharose column (0.75 × 2 cm). The column was washed with 50 mM potassium phosphate and 1 mM EDTA (Buffer B) until all unbound *N*′-(7-nitrobenz-2-oxa1,3-diazol-4-yl)ethylenediamine (NBD) had been removed. The NBD-labelled protein was then eluted with buffer B containing 1 M sodium chloride and 10 μM 20α-hydroxycholesterol. The concentrations of NBD and CYP11A1 were determined spectrophotometrically, with extinction coefficients of 27,300 [39] and 110,000 M^{-1} cm^{-1} at 478 and 404 nm, respectively. The NBD concentration was calculated after correction for the absorbance contribution due to CYP11A1 at 478 nm.

2.10. Half-time for vesicle association and steady state fluorescence

The fluorescence for soluble and vesicle-bound CYP11A1-NBD was measured in a stirred cuvette at 20 °C with excitation at 480 nm and emission at 535 nm with 5-nm bandwidths. The fluorescence was corrected for scatter as described for tryptophan fluorescence and the ratio of membrane-bound to soluble fluorescence intensity was determined for the NBD-labelled wild-type and mutant

cytochromes CYP11A1. Buffer, vesicle and CYP11A1 concentrations were as for measurements of acrylamide quenching of tryptophan fluorescence except the vesicles comprised of egg phosphatidylcholine, 20α-hydroxycholesterol and cardiolipin in a molar ratio of 1:0.15:0.15. The fluorescence intensity was measured as a function of time from the addition of vesicles and a single exponential curve was fitted for the fluorescence change for the combined data of duplicate experiments for each CYP11A1 mutant. A small change (2%) in fluorescence due to vesicle scatter occurred following mixing of CYP11A1-NBD and vesicles but was very rapid and did not interfere with half-time measurements for CYP11A1-NBD association with vesicles. The half-time for the association of unlabelled CYP11A1 with vesicles containing cholesterol was also measured for some CYP11A1 mutants, using the spin state change that accompanies cholesterol binding [15,16]. Concentrations and conditions were as for measurement of tryptophan fluorescence.

3. Results

3.1. Hydrophobicity profiles of mitochondrial cytochromes P450

The multiply aligned interfacial hydrophobicity profiles of CYP11A1 and two other mitochondrial P450 enzymes are illustrated in Fig. 1. The labelled regions of the E, F, H and I helices, the F–G loop and β 2–1 and 2–2 are potential membrane interfacial binding regions for all three mitochondrial cytochromes CYP11A1, 11B1 and 27A1. The hydrophobicity trends are generally consistent for the mitochondrial cytochromes P450 although there are considerable differences in the amplitude of the Δ*G* predicted for localisation from water to membrane interface. Interestingly, the regions of common prediction are also consistently found in other mitochondrial cytochromes P450. The profile for the N-terminal and F–G loop of CYP27A1 is clearly different from the more similar profiles of CYP11A1 and CYP 11B1. In the case of CYP27A1, the A′ helix contains a series of phenylalanine residues that elevate the overall hydrophobicity of this region compared to the A′ helix of CYP11A1. The F–G loop region of CYP11A1 and 11B1 enzymes have an amphipathic character that results in reduced hydrophobicity compared with CYP27A1.

3.2. CYP11A1 model

The sequence alignment used for modelling CYP11A1 is shown in Fig. 2. The template only contains sequence that has resolved structure and therefore some residues are not present for the template sequence. The sequence alignment includes some minor adjustment to incorporate secondary structure predictions for CYP11A1. The B′ helix is not found in CYP2C5 but was predicted for the mitochondrial P450 isoforms examined (CYP11A1, 11B1, 24 and 27A1; results not shown) and therefore may be a secondary structure feature that will be present in these enzymes. The recently published mutagenesis and modelling study of CYP11A1 using CYP102 as template did include a B′ helix for CYP11A1 [23]. The putative F–G loop of

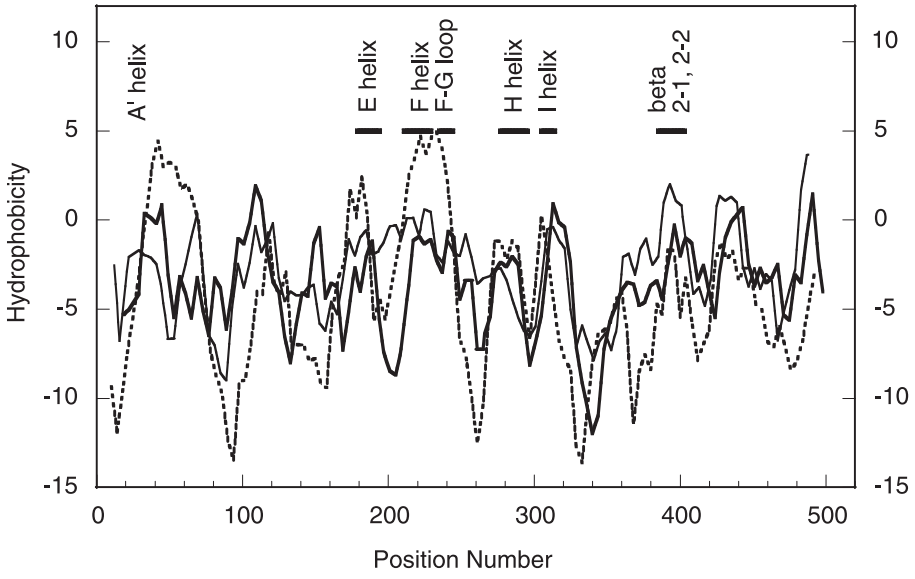

Fig. 1. Multiply aligned hydrophobicity profiles of mitochondrial cytochromes P450. The hydrophobicity scale of Wimley and White [20] was used for generation of the profiles with regions of sequence that have a favourable Δ*G* for membrane interfacial partitioning being indicated with a bar. Hydrophobicity values are for mature sequences of bovine CYP11A1 (thick solid line), human CYP11B1 (thin line) and human CYP27A1 (dashed line) and are plotted against the sequence number for the multiple alignment. Putative secondary structure features are labelled.

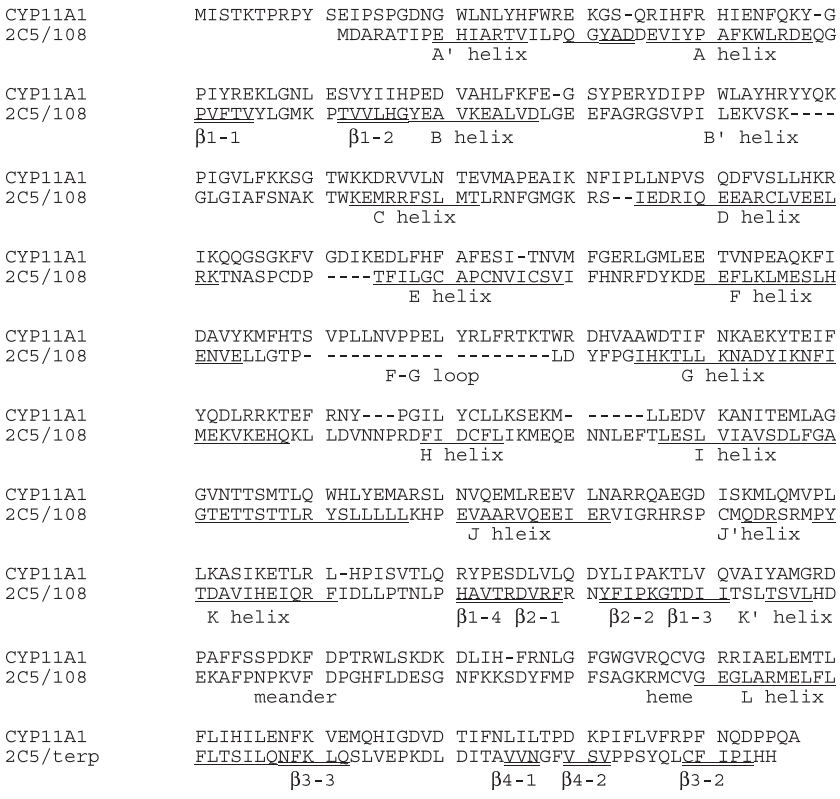

Fig. 2. Sequence alignment of CYP11A1 and the modelling template sequence of CYP2C5. Primary sequence was aligned for CYP11A1 and CYP2C5, except for the A′ and A helix regions where the residues of CYP108 (1CPT.pdb) were used as template up to the C-terminal of the A helix. Alpha helices are underlined and beta sheet structures are double-underlined in the positions corresponding to the CYP2C5 structure (1DT6.pdb).

CYP11A1 did not contain significant homology to any structure known and was not predicted to have defined secondary structure. The F–G loop for CYP2C5 is approximately five residues shorter from the F helix to G-helix than that predicted for CYP11A1 and 10 of the residues for CYP2C5 were ambiguous in the crystal structure (Fig. 2). The sequence for the F–G loop region of CYP2C5 in particular is absent and Swiss-model has inserted a loop region from the loop database to accommodate the sequence length of CYP11A1. We consider the structure for this part of the molecule to be speculative but it is unlikely to traverse a membrane. The region most likely to interact with the membrane domain is the distal face of CYP11A1 shown in Fig. 3, which has an aromatic region surrounding a hydrophobic patch in the vicinity of the F–G loop. The CYP11A1 model highlighting tryptophan residues (space filled) that may be located within the putative membrane-binding domain is shown in Fig. 3. The proximal or adrenodoxin binding face of the CYP11A1 model has an overall positive charge. K338 and K342 have been implicated in adrenodoxin binding [23] but in our model these residues are recessed from the surface of the molecule, suggesting that they do not directly interact with adrenodoxin. These residues have a similar recessed location in the CYP11A1 model developed by Usanov et al. [23]. Other residues (K267, K403, K405 and R426) that are believed to be involved in adrenodoxin interaction [23] are all located on the proximal surface of our model. Our model is expected to have minor differences to the model of Usanov et al. [23] due to the different template structures used [40]. The major differences are likely to be within the distal face, in the regions of the B–C loop, the interior of the F and G helices, and beta sheet 4.

Procheck was used to analyse the stereochemical quality of the model. The results for the CYP11A1 model indicate that over 73% of residues are in the most favoured regions of the Ramachandran plot and 2.4% in disallowed regions while CYP2C5 had over 71% in allowed and 1.8% in disallowed regions. The model appears to be consistent with available data on CYP11A1 and stereochemistry is of comparable quality to the template. We consider the model as a useful tool for identification of the membrane-binding or distal domain of CYP11A1. The sites for deletion mutations were at the N- and C-terminal and the cysteine mutants were chosen within the A′ helix, B′ helix, F–G loop, G helix and in the beta sheet region at the C-terminal of CYP11A1. The E, H and I helices were not analysed because they do not appear on the distal surface of our CYP11A1 model. The A′ helix was investigated for possible membrane interaction because it is located at the

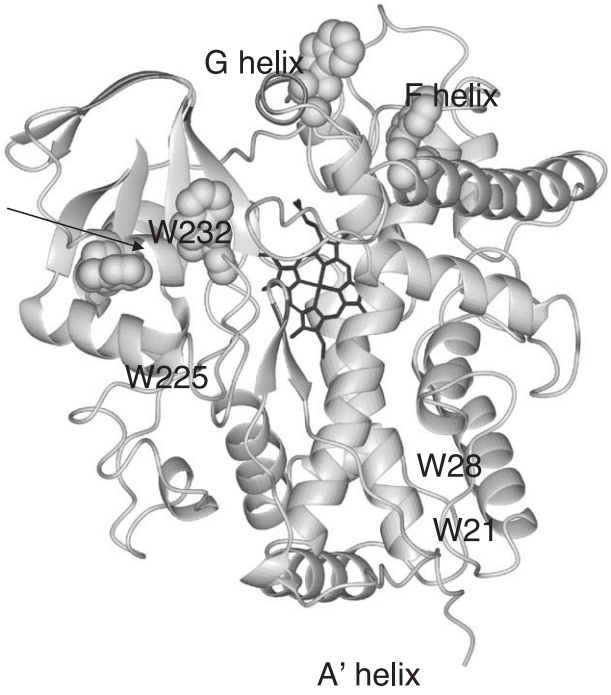

Fig. 3. Modelled Structure of CYP11A1. A ribbon diagram of the CYP11A1 model structure viewed from the distal surface that is putatively the membrane binding domain (approximately parallel to the plane of the figure). The heme is roughly parallel to the membrane domain and tryptophan residues located on the distal surface are space filled. Some of the relevant secondary structures are labelled. The diagram was prepared with MolMol [51].

position of the hydrophobic N-terminal anchor of the microsomal cytochromes P450. The B′ helix has been previously implicated in cholesterol interaction [41] and, from our model, is located on the putative membrane-binding face of cytochrome CYP11A1.

3.3. Characterisation of CYP11A1 mutants

The N- and C-terminal deletion mutants were expressed as spectrally stable, low spin enzyme in *E. coli* membranes, but were unstable during recording of the CO-reduced minus reduced difference spectra where partial denaturation to P420 occurred. These mutants proved to be unstable during extraction and purification. Most of the cysteine mutants were stable as judged from their CO-reduced minus reduced difference spectra and we typically purified 100 to 200 nmol from 1 l of culture. The expressed mutants that were unstable and therefore not purified in sufficient quantities for fluorescence analysis were H26C, Y200C, D233C and L470C. Y200C and L470C were denatured during extraction and purification. The mutant N23C was expressed and purified but found to be unstable during chemical labelling with IANBD. To test their structural integrity, all mutants that were purified, including N23C, H26C and D233C, were examined for their ability to display a type 1 spectral response (a shift to a higher spin state) in response to binding cholesterol from the vesicle membrane. All mutants displayed a typical type 1 response (data not shown), indicating they can access membrane cholesterol and have a functional active site in terms of the spin state of the heme. To further check structural integrity, we measured the maximum velocity of wild-type CYP11A1 and key mutants including C264S, L58C, V212C, L219C, V229C, and N237C, which all had turnover numbers (k_{cat}) of approximately 20 min^{-1}, similar to that of the native enzyme purified from bovine adrenals (17 min^{-1}). The L460C mutant had a very low turnover number of 0.5 min^{-1}. Other mutants were not tested for activity. C264S, V212C, L219C and V229C had half-times of 3.5 to 4 min for association with vesicles containing cholesterol, measured from the spin-state change. Both expressed wild-type CYP11A1 and C264S had K_m values for adrenodoxin of 1.6 ± 0.2 μM.

3.4. Distribution of CYP11A1 between the membrane and soluble fractions of E. coli

The distribution of microsomal P450 enzymes has been assessed by fractionation of *E. coli* into soluble and membrane fractions following the truncation of the N-terminal hydrophobic anchor [32,42]. In a similar approach, mutants of mitochondrial cytochrome P45027A1 were analysed by Western blot analysis following *E. coli* fractionation in order to identify critical residues involved in membrane binding [43,44]. We have likewise made use of Western blot analysis to measure the effect of CYP11A1 N- and C-terminal deletion mutations on membrane localisation (Fig. 4). The *E. coli* membranes of the expressed wild type, A′ helix deletion and C-terminal deletion (I468STOP) mutants of CYP11A1 contained $76 \pm 13\%$, $47 \pm 9\%$ and $86 \pm 18\%$ of the combined membrane and cytosolic CYP11A1 content, respectively. The amount of CYP11A1 detected in the inclusion body fraction was approximately 12% for the wild type and both deletion mutants. Two separate experiments analysed in triplicate gave similar results, indicating decreased membrane association of the A′ helix deletion mutant and no change in localisation of the C-terminal deletion mutant compared to wild-type CYP11A1.

3.5. Steady-state tryptophan fluorescence of membrane associated CYP11A1

Soluble CYP11A1 has an emission maximum at approximately 338 nm for the excitation of tryptophan residues at 295 nm. This maximum is indicative of relatively non-polar tryptophan residues as observed by others [6,45]. For vesicle-associated CYP11A1 where tryptophan fluorescence has not been measured before, the emission maximum was at 337 nm, similar to the soluble enzyme. This implies that there is no major change in average hydrophobicity of the nine tryptophan residues

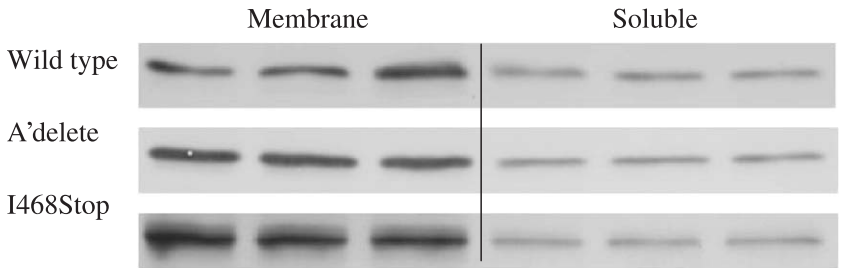

Fig. 4. Western blot analysis of the distribution of N- and C-terminal deletion mutants of CYP11A1 between membrane and soluble fractions of *E. coli*. Following fractionation, triplicates of samples were subjected to SDS-PAGE, transferred to nitrocellulose and probed with anti-bovine CYP11A1 antiserum. Amounts of sample applied were: wild type, 2 μg membrane, 10 μg soluble; A' delete, 2 μg membrane, 2 μg soluble; I468STOP, 10 μg membrane, 20 μg soluble fraction.

of CYP11A1 upon association with the phospholipid membrane.

3.6. Tryptophan fluorescence quenching by acrylamide

CYP11A1 in solution and in vesicles gave a linear plot of F_0/F versus $[Q]$, suggesting a single type of quenching mechanism by acrylamide. There were typical quench constants (K_{sv}) of 2.12 ± 0.04 M^{-1} for soluble CYP11A1 and 1.88 ± 0.04 M^{-1} for vesicle associated enzyme (Fig. 5A). The number of accessible tryptophan residues was significantly reduced ($P < 0.05$) from 8.6 ± 0.7 to 7.0 ± 0.4 for the membrane-bound enzyme when compared with soluble enzyme (Fig. 5B). The soluble enzyme has previously been observed to have a dynamic quenching mechanism with quench constant of 1.52 M^{-1} at 20 °C with essentially all nine tryptophan residues exposed to acrylamide quenching [45]. Our results indicate that at least one and more likely two of the quenchable tryptophan residues of soluble CYP11A1 become inaccessible to acrylamide quenching following membrane association.

3.7. Half-time for the CYP11A1-NBD fluorescence change associated with incorporation into vesicles

The fluorescence of soluble CYP11A1-NBD was low for all mutants and increased with time following the addition of vesicles in a manner giving a good fit to a single exponential curve, indicating a first-order or pseudo-first-order process (Fig. 6). A single exponential curve gave a superior fit to a bi-exponentional function, which was also tested. The fluorescence change appears to give a measure of the rate of association of the protein with the vesicles (see Discussion). Similar measurements have been used to characterize the rate of association of other proteins with membranes and to determine the rate of ligand binding [39,46,47]. The wild-type CYP11A1-NBD was estimated to have a half-time of approximately 0.8 min for the fluorescence change following mixing with phosphatidylcholine vesicles containing 20α-hydroxycholesterol. Two F–G loop mutants, V212C-NBD and L219C-NBD, had significant increases in the half-time for the fluorescence change

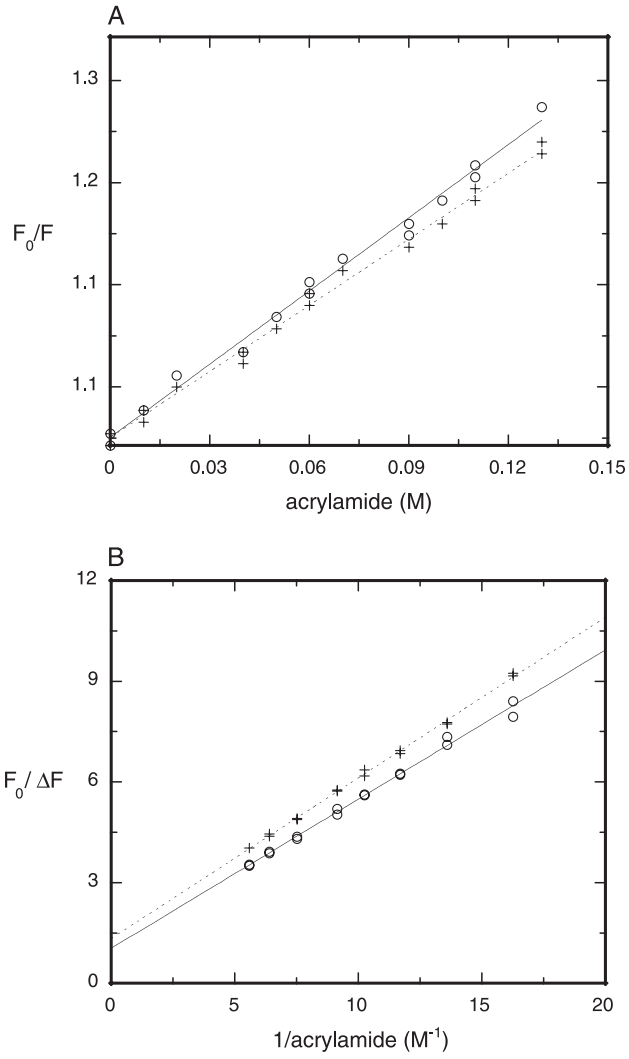

Fig. 5. Tryptophan fluorescence quenching in the presence and absence of phosphatidylcholine vesicles. (A) Acrylamide quenching of tryptophan residues of soluble (circles) and membrane-associated CYP11A1 (crosses) were analysed using the Stern–Volmer plot. (B) Lehrer plot of tryptophan fluorescence change versus the inverse of acrylamide concentration. The intercept on the $F_0/\Delta F$ axis gives the inverse of the fraction of accessible tryptophan residues for the soluble (circles) and vesicle-bound (crosses) CYP11A1.

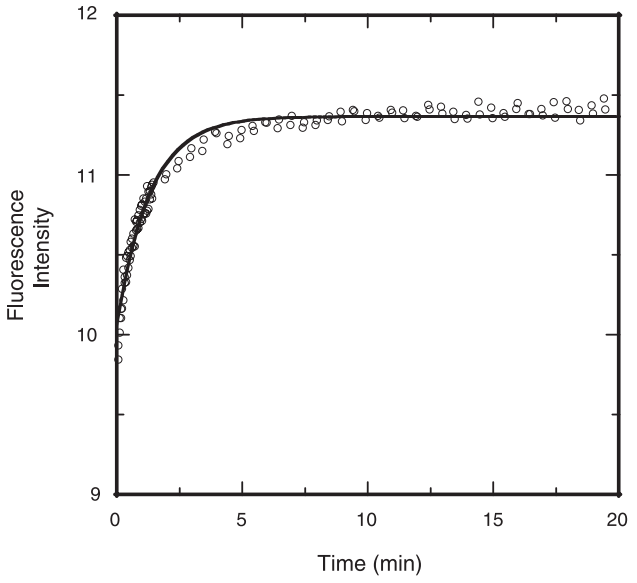

Fig. 6. Time course for the change in NBD fluorescence with association of CYP11A1 with vesicles. Fluorescence of NBD-labelled CYP11A1 (0.5 μM) was monitored during the association of CYP11A1 with small unilamellar vesicles. Fluorescence (excitation 480 nm and emission 535 nm) was measured at 20 °C in a stirred quartz cuvette with a path length of 5 mm. A single exponential curve was fitted to the data.

following mixing with vesicles (Fig. 7). These mutations occur in the putative F–G loop of CYP11A1 and showed a 2- to 2.5-fold increase in half-time compared with those for wild-type CYP11A1-NBD. Other CYP11A1 mutants that we tested did not have significantly different half-times to that for wild-type CYP11A1.

3.8. Relative fluorescence of P450-NBD in solution and in the presence of vesicles

After membrane incorporation was complete, the ratio of relative fluorescence in vesicle to the relative fluorescence of soluble CYP11A1-NBD (F(vesicle/soluble)) was significantly increased for V212C-NBD and L219C-NBD compared to wild-type CYP11A1-NBD. The low fluorescence of the NBD-labelled P450 mutants in solution indicates that the environmentally sensitive NBD exists in a relatively hydrophilic environment. The increase in fluorescence observed for V212C-NBD and L219C-NBD indicates the NBD is localised to a more hydrophobic environment following membrane association. This is consistent with aqueous exposed NBD becoming buried within the acyl chain region of the phospholipids as the CYP11A1 incorporates into the vesicle membrane. The low emission maxima for the V212C-NBD and L219C-NBD (Fig. 8) indicate that the soluble enzyme provides a relatively hydrophobic environment for the bound NBD. Following membrane binding, there is a blue shift in emission that indicates an even more hydrophobic environment for the bound NBD which is also consistent with the relocation of residues V212C and L219C into the hydrophobic acyl chains of the membrane. As the distance from the F–G loop increases, mutations predicted to be in the G helix (V229C, T234C, N237C and T243C) show increasing hydrophilic exposure as indicated by the NBD emission maxima (Fig. 8). G helix residues show a moderate blue shift following membrane association of the NBD labelled CYP11A1 mutants, which demonstrates a sensitivity to binding, but not a change in exposure, to the quenching

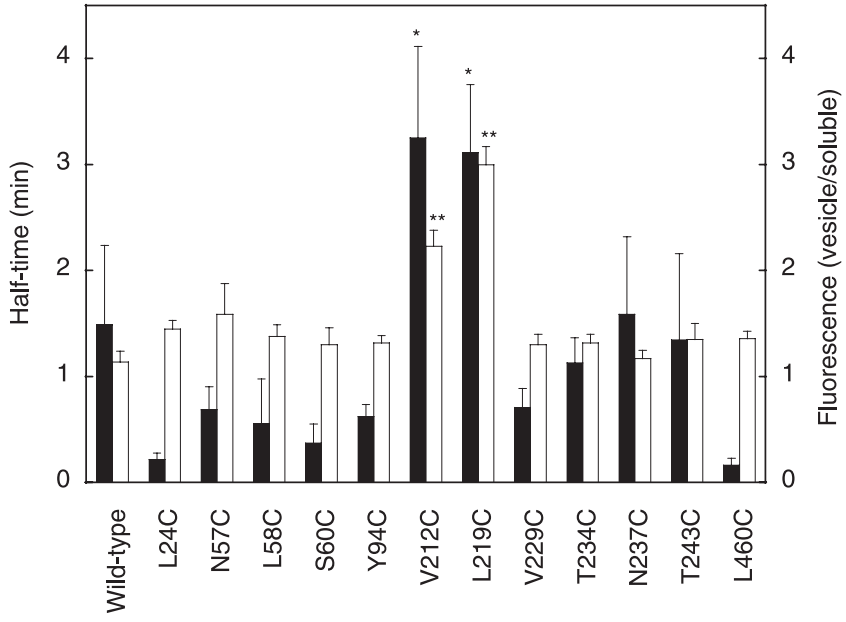

Fig. 7. Fluorescence characteristics of CYP11A1 cysteine mutants labelled with NBD. Filled bars are the half-times for the increase in fluorescence following addition of phospholipid vesicles to soluble CYP11A1. Error bars are ± standard deviation of the curve fit for two combined experiments. Open bars are the ratio of relative fluorescence of membrane bound to soluble CYP11A1. Error bars are ± standard deviation of 4 experiments. Results with significant difference for $P<0.05$ or $P<0.005$ from wild type are marked with * or **, respectively.

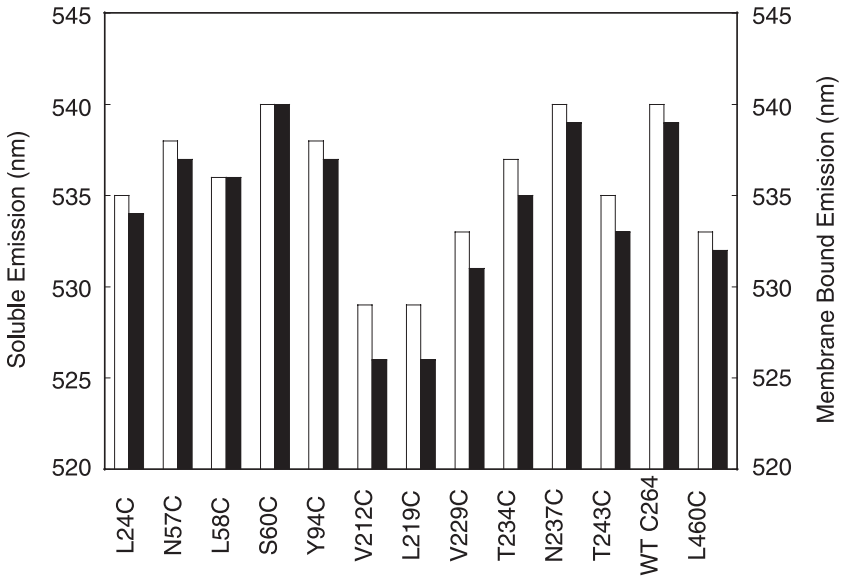

Fig. 8. Fluorescence emission characteristics of CYP11A1 cysteine mutants labelled with NBD. Open and filled bars represent the emission maxima for soluble NBD-CYP11A1 and membrane-bound NBD-CYP11A1, respectively. The excitation maximum was 480 nm with emission scanned from 500 to 600 nm at a rate of 120 nm/min. Other conditions were as for Fig. 6.

action of water. Other regions of the protein appear less affected by membrane binding than the F–G loop and G helix.

4. Discussion

A common first step to identifying membrane domains of proteins is to estimate the hydrophobicity of the primary sequence using available prediction algorithms. While topology prediction has correctly identified an N-terminal membrane anchor in microsomal P450s, no transmembrane segment was predicted for CYP11A1 using either the Engleman or Kyte and Doolittle scales of hydrophobicity [4]. Experimental evidence indicates that CYP11A1 is not likely to be transmembrane but is membrane-bound through hydrophobic interaction. The hydrophobicity plot in Fig. 1 was generated with the hydrophobicity scale of Wimley and White [21] and several possible interfacial membrane domains were predicted for the mitochondrial cytochromes P450. The Wimley–White hydropathy scale predicts membrane proteins with up to 99% accuracy by accounting for the energetic cost of burying an entire residue within a membrane or membrane interface environment rather than just the side chain of the residue. We made use of this algorithm to assist with identification of hydrophobic stretches of amino acids that may be involved in membrane binding but that do not necessarily span the membrane. Hydrophobicity scales can result in false predictions, as has been reported for some internal hydrophobic helices of extramembrane proteins [48]. Most notably, the I helix is unlikely to interact with the membrane and is almost certainly an internal hydrophobic helix, as observed for the highly conserved tertiary structure seen for CYP101, CYP108, CYP107A, CYP102, CYP2C5, and CYP51. Analysis of the hydropathy profile in Fig. 1 for interfacial membrane binding of mitochondrial P450 enzymes in the regions of the predicted A′ helix and F–G loop reveals elevated hydrophobicity of CYP27A1. Expression studies on CYP27A1 have shown that it is entirely associated with the membrane fraction of *E. coli* cells [44] while we have shown that only 75% of CYP11A1 is associated with the membranes. As noted by Murtazina et al. [44], CYP27A1 requires higher detergent concentrations for solubilisation from the membrane compared with that required for CYP11A1 solubilisation. This may explain the greater relative hydrophobic interaction seen experimentally [44]. The reduced hydrophobicity of CYP11A1 compared with other mitochondrial P450 enzymes, and in particular CYP27A1, may facilitate crystallisation of this enzyme. In the case of CYP2C5, crystallisation of the enzyme followed the introduction of mutations that induced monomerisation of the enzyme [12,22]. Further work is required with the mitochondrial P450 enzymes to explore the potential gains a similar approach might provide.

Evaluation of our molecular model of CYP11A1 in concert with hydrophobicity profiles gives rise to the hypothesis that the A′ helix and the F–G loop region are involved in membrane binding. In the absence of a transmembrane domain, it appears reasonable to suggest that the A′ helix would lie within the interfacial region of the membrane lipids. The reduced proportion of CYP11A1 associated with the *E. coli* membrane fraction for the A′ helix deletion mutant supports this hypothesis. We made three cysteine mutants to examine this hypothesis further, only to find that H26C was unstable and could not be purified, N23C was stable enough

to purify but was unstable during NBD labelling conditions and only L24C was stable for purification and labelling with NBD. The environmentally sensitive NBD bound to L24C gave no evidence of being buried in a hydrophobic environment in the presence of vesicles. This mutant gave a typical high spin transition when added to vesicles containing cholesterol, indicating vesicle association had occurred. The A′ helix is almost certainly found on the surface of CYP11A1 but further study is required to determine whether it is involved in membrane interaction. There is only moderate sequence identity among the mitochondrial cytochromes P450 within the A′ helix, whereas there is high sequence identity in this region for cytochromes CYP11A1 and 11B1 for all species with known sequence (results not shown). Our results show that two out of three mutations within the putative A′ helix caused structural instability of CYP11A1, indicating an important structural role for this region of the molecule that may be specific to CYP11A1 and closely related mitochondrial cytochromes P450.

Cysteine mutagenesis and NBD labelling strongly support the hypothesis that the F–G loop region of CYP11A1 is embedded in the hydrophobic membrane domain. The F–G loop mutants V212C and L219C gave increased NBD fluorescence upon vesicle association, indicating a shift to a more hydrophobic environment. This is the first time that it has been shown that residues of the F–G loop of a mitochondrial cytochrome P450 integrate into the membrane environment. Residue V229 and other residues C-terminal of this that are probably located in the G helix, do not appear to be located in the hydrophobic membrane domain but are sensitive to membrane association. Our evidence therefore suggests that unless there are gross conformational differences between the known P450 structures and CYP11A1 in the vicinity of the F helix, then there is not a long enough stretch of amino acids in the F–G loop to generate a transmembrane domain. This is in support of the major body of evidence indicating a monotopic association of CYP11A1 with vesicles [9,10].

As well as showing increased NBD fluorescence and relocation to a more hydrophobic environment, the F–G loop mutants V212C and L219C displayed a slower rate of fluorescence change than wild-type CYP11A1 on mixing with vesicles. We have previously measured the rate of incorporation of CYP11A1 into phospholipid vesicles from the change in spin state that accompanies cholesterol binding or dissociation [15]. Using this technique, we checked the rate of association with vesicles of unlabelled wild-type CYP11A1 as well as the V212C and L219C mutants and found that their half-times were similar (results not shown). Half-times were slower than for the fluorescence change of NBD-labelled wild-type CYP11A1 following mixing with vesicles but were similar to the values for NBD-labelled V212C and L219C. We suggest that the fluorescence change observed for NBD-labelled V212C and L219C provides a measure of the rate of integration of the CYP11A1 into the hydrophobic membrane phase while the fluorescence change for NBD-labelled wild-type CYP11A1 and the other mutants examined measures peripheral association with the membrane, but not integration. This interpretation is supported by studies on colicin association with vesicles, which was examined using cysteine mutagenesis with subsequent labelling and EPR analysis [46]. Colicin showed a rapid initial association with vesicles followed by a slower insertion phase and the two events could be distinguished by the position of the labelled residue in the protein.

We have detected a change in environment of tryptophan residues of CYP11A1 upon membrane association consistent with the important function aromatic amino acids play in membrane interfacial binding [49,50]. Examination of our model structure indicates that four of the nine tryptophan residues are located on the distal face of CYP11A1. We can therefore predict that the two tryptophan residues detected to have reduced exposure to acrylamide due to membrane association could be any two of W21, W28 of the A′ helix and W225 and W232 of the F–G loop and G helix. We cannot exclude the involvement of all four tryptophan residues in membrane association but only an average of approximately two of these have altered accessibility to the aqueous fluorescence quencher, acrylamide. Our results from cysteine mutagenesis and labelling reveal that V212 and L219 are membrane-integrated while the nearby residues V229, T234, N237 and T243 are not. From this and our model structure, it seems possible that W225 is integrated within the membrane, being in closest proximity to L219. The residue W232 is less likely to be integrated because it is located between residues that are not within in the hydrophobic membrane domain.

Our data suggest that the F–G loop region is the primary site of interaction of mitochondrial P450s with the membrane. Unlike mitochondrial cytochromes P450, microsomal P450 enzymes have a primary site of membrane interaction in the form of a single transmembrane anchor at the N-terminal [14]. There is evidence that the F–G loop is a secondary site of interaction of microsomal P450s with the membrane [50]. The mitochondrial P450 enzymes have an extended F–G loop region compared to microsomal P450s, which acts to provide an improved ΔG that can in part compensate for the absence of a transmembrane anchor. It remains to be seen if additional regions of CYP11A1 and other mitochondrial cytochromes P450 are buried within the membrane.

Acknowledgements

We thank Dr. Kevin Croft from the University of Western Australia, Department of Medicine, for the use of the fluorometer, Dr. Dharharajan for the cDNA for bovine CYP11A1 and Dr. Guido Pintacuda for assistance with the program MolMol. We also thank Dr. Eric Johnson for providing the coordinates of CYP2C5 prior to their release through the Research Collaboratory for Structural Bioinformatics Protein Databank. This work was supported by a University of Western Australia Small Grant (to RCT).

References

[1] D.W. Seybert, J.J. Lancaster, J.D. Lambeth, H. Kamin, Participation of the membrane in the side chain cleavage of cholesterol. Reconstitution of cytochrome P-450scc into phospholipid vesicles, J. Biol. Chem. 254 (1979) 12088–12098.

[2] H. Blum, J.S. Leigh, J.C. Salerno, T. Ohnishi, The orientation of bovine adrenal cortex cytochrome P-450 in submitochondrial particle multilayers, Arch. Biochem. Biophys. 187 (1978) 153–157.

[3] H. Kamin, C. Batie, J.D. Lambeth, J. Lancaster, L. Graham, J.C. Salerno, Paramagnetic probes of multicomponent electron-transfer systems, Biochem. Soc. Trans. 13 (1985) 615–618.

[4] D.R. Nelson, H.W. Strobel, On the membrane topology of vertebrate cytochrome P-450 proteins, J. Biol. Chem. 263 (1988) 6038–6050.

[5] G. Vergeres, K.H. Winterhalter, C. Richter, Identification of the membrane anchor of microsomal rat liver cytochrome P-450, Biochemistry 28 (1989) 3650–3655.

[6] P. Anzenbacher, J. Hudecek, S. Vajda, V. Fidler, C. Larroque, R. Lange, Nanosecond fluorescence of tryptophans in cytochrome P-450scc (CYP11A1): effect of substrate binding, Biochem. Biophys. Res. Commun. 181 (1991) 1493–1499.

[7] S.A. Usanov, A.A. Chernogolov, V.L. Chashchin, Is cytochrome P-450scc a transmembrane protein? [published erratum appears in FEBS Lett 1991 Mar 25;280(2):400] FEBS Lett. 275 (1990) 33–35.

[8] P.F. Churchill, T. Kimura, Topological studies of cytochromes P-450scc and P-45011 beta in bovine adrenocortical inner mitochondrial membranes. Effects of controlled tryptic digestion, J. Biol. Chem. 254 (1979) 10443–10448.

[9] D. Schwarz, V. Kruger, A.A. Chernogolov, S.A. Usanov, A. Stier, Rotation of cytochrome P450SCC (CYP11A1) in proteoliposomes studied by delayed fluorescence depolarization, Biochem. Biophys. Res. Commun. 195 (1993) 889–896.

[10] D. Schwarz, W. Richter, V. Kruger, A. Chernogolov, S. Usanov, A. Stier, Direct visualization of a cardiolipin-dependent cytochrome P450scc-induced vesicle aggregation, J. Struct. Biol. 113 (1994) 207–215.

[11] W.J. Ou, A. Ito, K. Morohashi, Y. Fujii-Kuriyama, T. Omura, Processing-independent in vitro translocation of cytochrome P-450(SCC) precursor across mitochondrial membranes, J. Biochem. (Tokyo) 100 (1986) 1287–1296.

[12] P.A. Williams, J. Cosme, V. Sridhar, E.F. Johnson, D.E. McRee, Mammalian microsomal cytochrome P450 monooxygenase: structural adaptations for membrane binding and functional diversity, Mol. Cell 5 (2000) 121–131.

[13] S.J. Pernecky, N.M. Olken, L.L. Bestervelt, M.J. Coon, Subcellular localization, aggregation state, and catalytic activity of microsomal P450 cytochromes modified in the NH2-terminal region and expressed in *Escherichia coli*, Arch. Biochem. Biophys. 318 (1995) 446–456.

[14] M.L. Shank-Retzlaff, G.M. Raner, M.J. Coon, S.G. Sligar, Membrane topology of cytochrome P450 2B4 in Langmuir–Blodgett monolayers, Arch. Biochem. Biophys. 359 (1998) 82–88.

[15] R.C. Tuckey, H. Kamin, Kinetics of the incorporation of adrenal cytochrome P-450scc into phosphatidylcholine vesicles, J. Biol. Chem. 257 (1982) 2887–2893.

[16] P. Kisselev, R. Wessel, S. Pisch, U. Bornscheuer, R.D. Schmid, D. Schwarz, Branched phosphatidylcholines stimulate activity of cytochrome P450SCC (CYP11A1) in phospholipid vesicles by enhancing cholesterol binding, membrane incorporation, and protein exchange, J. Biol. Chem. 273 (1998) 1380–1386.

[17] J.D. Lambeth, D.W. Seybert, H. Kamin, Phospholipid vesicle-reconstituted cytochrome P-450SCC. Mutually facilitated binding of cholesterol and adrenodoxin, J. Biol. Chem. 255 (1980) 138–143.

[18] D. Schwarz, P. Kisselev, R. Wessel, O. Jueptner, R.D. Schmid, Alpha-branched 1,2-diacyl phosphatidylcholines as effectors of activity of cytochrome P450SCC (CYP11A1). Modeling the structure of the fatty acyl chain region of cardiolipin, J. Biol. Chem. 271 (1996) 12840–12846.

[19] M.J. Headlam, R.C. Tuckey, The effect of glycerol on cytochrome P450scc (CYP11A1) spin state, activity, and hydration, Arch. Biochem. Biophys. 407 (2002) 95–102.

[20] C. Notredame, D.G. Higgins, J. Heringa, T-Coffee: a novel method for fast and accurate multiple sequence alignment, J. Mol. Biol. 302 (2000) 205–217.

[21] W.C. Wimley, S.H. White, Experimentally determined hydrophobicity scale for proteins at membrane interfaces, Nat. Struct. Biol. 3 (1996) 842–848.

[22] J. Cosme, E.F. Johnson, Engineering microsomal cytochrome P450 2C5 to be a soluble, monomeric enzyme. Mutations that alter aggregation, phospholipid dependence of catalysis, and membrane binding, J. Biol. Chem. 275 (2000) 2545–2553.

[23] S.A. Usanov, S.E. Graham, G.I. Lepesheva, T.N. Azeva, N.V. Strushkevich, A.A. Gilep, R.W. Estabrook, J.A. Peterson, Probing the interaction of bovine cytochrome P450scc (CYP11A1) with adrenodoxin: evaluating site-directed mutations by molecular modeling, Biochemistry 41 (2002) 8310–8320.

[24] A. Wada, M.R. Waterman, Identification by site-directed mutagenesis of two lysine residues in cholesterol side chain cleavage cytochrome P450 that are essential for adrenodoxin binding, J. Biol. Chem. 267 (1992) 22877–22882.

[25] T. Maniatis, E.F. Fritsch, J. Sambrook, Molecular Cloning. A Laboratory Manual, Cold Spring Harbor Laboratory, New York, NY, 1982.

[26] S.T. Woods, J. Sadleir, T. Downs, T. Triantopoulos, M.J. Headlam, R.C. Tuckey, Expression of catalytically active human cytochrome P450scc in *Escherichia coli* and mutagenesis of isoleucine-462, Arch. Biochem. Biophys. 353 (1998) 109–115.

[27] G.I. Lepesheva, T.N. Azeva, N.V. Strushkevich, T.B. Adamovich, T.S. Cherkesova, S.A. Usanov, Comparative structural–functional characterization of recombinant and natural adrenodoxin. Interaction with cytochrome P450scc, Biochemistry (Mosc.) 64 (1999) 1079–1088.

[28] R.C. Tuckey, P.M. Stevenson, Properties of bovine luteal cytochrome P-450scc incorporated into artificial phospholipid vesicles, Int. J. Biochem. 16 (1984) 497–503.

[29] G.I. Lepesheva, S.A. Usanov, Comparative structural and immunochemical characterization of recombinant and natural cytochrome P450scc (CYPXIAI), Biochemistry (Mosc.) 63 (1998) 224–234.

[30] T. Omura, R. Sato, The carbon monoxide-binding pigment of liver microsomes: I. Evidence for its hemoprotein nature, J. Biol. Chem. 239 (1964) 2370–2378.

[31] R.C. Tuckey, K.J. Cameron, Side-chain specificities of human and bovine cytochromes P-450scc, Eur. J. Biochem. 217 (1993) 209–215.

[32] E.M. Gillam, T. Baba, B.R. Kim, S. Ohmori, F.P. Guengerich, Expression of modified human cytochrome P450 3A4 in *Escherichia coli* and purification and reconstitution of the enzyme, Arch. Biochem. Biophys. 305 (1993) 123–131.

[33] O.H. Lowry, N.J. Rosebrough, A.L. Farr, R.J. Randall, Protein measurement with the folin phenol reagent, J. Biol. Chem. 193 (1951) 265–275.

[34] R.C. Tuckey, J. Sadleir, The concentration of adrenodoxin reductase limits cytochrome P450scc activity in the human placenta, Eur. J. Biochem. 263 (1999) 319–325.

[35] R.C. Tuckey, Z. Kostadinovic, P.M. Stevenson, Ferredoxin and cytochrome P-450scc concentrations in granulosa cells of porcine ovaries during follicular cell growth and luteinization, J. Steroid Biochem. 31 (1988) 201–205.

[36] D.B. Calhoun, J.M. Vanderkooi, S.W. Englander, Penetration of small molecules into proteins studied by quenching of phosphorescence and fluorescence, Biochemistry 22 (1983) 1533–1539.

[37] S.S. Lehrer, Solute perturbation of protein fluorescence. The quenching of the tryptophyl fluorescence of model compounds and of lysozyme by iodide ion, Biochemistry 10 (1971) 3254–3263.

[38] K. Gekko, S.N. Timasheff, Thermodynamic and kinetic examina-

tion of protein stabilization by glycerol, Biochemistry 20 (1981) 4677–4686.
[39] Q. Wang, D. Cui, Q. Lin, Fluorescence studies on the interaction of a synthetic signal peptide and its analog with liposomes, Biochim. Biophys. Acta 1324 (1997) 69–75.
[40] P.A. Williams, J. Cosme, V. Sridhar, E.F. Johnson, D.E. McRee, Microsomal cytochrome P450 2C5: comparison to microbial P450s and unique features, J. Inorg. Biochem. 81 (2000) 183–190.
[41] I.A. Pikuleva, R.L. Mackman, N. Kagawa, M.R. Waterman, P.R. Ortiz de Montellano, Active-site topology of bovine cholesterol side-chain cleavage cytochrome P450 (P450scc) and evidence for interaction of tyrosine 94 with the side chain of cholesterol, Arch. Biochem. Biophys. 322 (1995) 189–197.
[42] K. Nakayama, A. Puchkaev, I.A. Pikuleva, Membrane binding and substrate access merge in cytochrome P450 7A1, a key enzyme in degradation of cholesterol, J. Biol. Chem. 276 (2001) 31459–31465.
[43] I.A. Pikuleva, A. Puchkaev, I. Bjorkhem, Putative helix F contributes to regioselectivity of hydroxylation in mitochondrial cytochrome P450 27A1, Biochemistry 40 (2001) 7621–7629.
[44] D. Murtazina, A.V. Puchkaev, C.H. Schein, N. Oezguen, W. Nanavati, A. Nanavati, I.A. Pikuleva, Membrane–protein interactions contribute to efficient 27-hydroxylation of cholesterol by mitochondrial cytochrome P450 27A1, J. Biol. Chem. 17 (2002) 37582–37589.
[45] R. Lange, P. Anzenbacher, S. Muller, L. Maurin, C. Balny, Interaction of tryptophan residues of cytochrome P450scc with a highly specific fluorescence quencher, a substrate analogue, compared to acrylamide and iodide, Eur. J. Biochem. 226 (1994) 963–970.
[46] Y.K. Shin, C. Levinthal, F. Levinthal, W.L. Hubbell, Colicin E1 binding to membranes: time-resolved studies of spin-labeled mutants, Science 259 (1993) 960–963.
[47] U. Gether, S. Lin, B.K. Kobilka, Fluorescent labeling of purified beta 2 adrenergic receptor. Evidence for ligand-specific conformational changes, J. Biol. Chem. 270 (1995) 28268–28275.
[48] S. Jayasinghe, K. Hristova, S.H. White, Energetics, stability, and prediction of transmembrane helices, J. Mol. Biol. 312 (2001) 927–934.
[49] J.A. Killian, G. von Heijne, How proteins adapt to a membrane–water interface, TIBS 25 (2000) 429–434.
[50] A.S. Ladokhin, S.H. White, Protein chemistry at membrane interfaces: non-additivity of electrostatic and hydrophobic interactions, J. Mol. Biol. 309 (2001) 543–552.
[51] R. Koradi, M. Billeter, K. Wuthrich, MOLMOL: a program for display and analysis of macromolecular structures, J. Mol. Graph. 14 (1996) 51–55.